

Anomalous Magnetic Properties of the Bilayered $\text{LaSr}_2\text{Mn}_{2-z}\text{Co}_z\text{O}_7$ ($z = 0-0.15$) Manganite

M.H. Ehsani · M.E. Ghazi · P. Kameli · F.S. Razavi

Received: 16 December 2012 / Accepted: 19 February 2013 / Published online: 16 March 2013
© Springer Science+Business Media New York 2013

Abstract The Co-doped bilayered $\text{LaSr}_2\text{Mn}_2\text{O}_7$ manganite at low Co concentrations (0–0.15) was synthesized by the sol–gel process. The X-ray diffraction (XRD) technique confirms phase formation for all the samples under investigation. The results of ac magnetic susceptibility measurements indicate the effect of Co doping on the magnetic ordering phases. The indications of charge ordering (CO) transitions were observed in all the prepared compounds. The CO magnetic phase transition temperature was observed systematically shift to lower temperatures as the Co concentration increases. There was an anomalous oscillating magnetic behavior in all samples with a few peaks before the CO temperature in the paramagnetic (PM) region so that with an increasing Co doping, the number of peaks and amplitude were decreased. Also, the ac susceptibility measurements were performed in the presence of an applied dc magnetic field to further study of this oscillating behavior.

Keywords Bilayered manganite · Co-doped · Charge ordering · Oscillating behavior

M.H. Ehsani · M.E. Ghazi (✉)
Department of Physics, Shahrood University of Technology,
Shahrood 36155-316, Iran
e-mail: ebrahim_ghazi@yahoo.com

M.H. Ehsani
Department of Physics, Semnan University, Semnan 35195-363,
Iran

P. Kameli
Department of Physics, Isfahan University of Technology,
Isfahan 84156-8311, Iran

F.S. Razavi
Department of Physics, Brock University, St. Catharines L2S3A1,
Canada

1 Introduction

It is well known that Mn-based Ruddlesden–Popper (RP) compounds with the general formula $(\text{La,Sr})_{n+1}\text{Mn}_n\text{O}_{3n+1}$ have a layered-type structure. In this formula, n is the number of MnO_2 layers that are separated by an additional $(\text{La}_{1-x}\text{Sr}_x)_2\text{O}_2$ blocking bilayer. The bilayered ($n = 2$) manganites $\text{La}_{2-2x}\text{Sr}_{1+2x}\text{Mn}_2\text{O}_7$ have attracted much attention due to a variety of emerging phenomena such as the colossal magnetoresistance effect, tunneling magnetoresistance, and fascinating electronic and magnetic properties [1, 2]. In such compounds, MnO_2 layers have ferromagnetic (FM) metallic interactions, arising from a double-exchange (DE) mechanism through $\text{Mn}^{+3}-\text{O}-\text{Mn}^{+4}$ bonds [3]. There are also different antiferromagnetic (AFM) phases between the adjacent layers in variation of the doping level x and temperature. Besides, the DE mechanism, Jahn–Teller effect, phase separation (PS) [4], AFM superexchange, charge-orbital ordering, and spin fluctuation [5] also play an important role in manganite systems. Also, due to the reduced dimensionality in these materials, considerable anisotropic properties have been observed [6]. $\text{LaSr}_2\text{Mn}_2\text{O}_7$ that has an equal amount (50 %) of Mn^{+3} and Mn^{+4} ions, similar to the 50 % doped charge ordered three-dimensional (3D) manganites ($n = \infty$), is also expected to show similar spin/charge ordering phenomena according to the Goodenough model [7]. In the half-doped bilayered manganite $\text{LaSr}_2\text{Mn}_2\text{O}_7$, there is a transition into the CE-type charge-orbital ordered state at ~ 225 K. This state starts melting at ~ 170 K, where the A-type AFM spin ordering begins to form. Below this temperature, magnetic spins are ferromagnetically aligned in the a – b plane; however, they coupled antiferromagnetically along the c -axis. In addition, the minor CE-AFM state was reported to coexist with the major A-AFM ordering state below 145 K and suppressed below ~ 100 K, but not completely [8–10].

Beside the above mentioned studies, the bilayered manganites $\text{La}_{2-2x}\text{Sr}_{1+2x}\text{Mn}_2\text{O}_7$ offers another unique opportunity to investigate the Mn-site doping by magnetic and nonmagnetic ions. It is known that Mn-site doping in perovskite manganites dramatically changes the magnetic and electrical properties due to the crucial role of Mn ions in manganites. The effect of doping by the transition elements (TEs) Cr, Fe, Co, Ni, Cu, and Zn on the electronic transport and magnetic properties in $\text{La}_{1.4}\text{Sr}_{1.6}\text{Mn}_2\text{O}_7$, has clearly been referenced [11]. These results have shown that except for Cr, all other doping, significantly shifts the magnetic and insulator-metal transition temperature (T_{IM}) to a lower temperature. Also, the effect of Cr doping on the bilayered manganite $\text{La}_{1.4}\text{Sr}_{1.6}\text{Mn}_2\text{O}_7$ has been investigated by Yu et al. [12]. They have observed that at low dopant values, Cr doping enhances the 3 dimensions (3D) magnetic transition temperature, T_C , as well as a slight decrease in the resistivity and saturation magnetization. Mn-site doping by a non-magnetic ion such as Cu and Al in $\text{La}_{1.4}\text{Sr}_{1.6}\text{Mn}_2\text{O}_7$ and $\text{LaSr}_2\text{Mn}_2\text{O}_7$ has shown that DE interaction between the mixed-valance Mn ions is suppressed, and transport behavior as well as magnetic properties are changed [13, 14].

Thus, study of the effects of Mn-site doping by the transition elements in bilayered manganite could be an interesting phenomenon. Among transition elements, Co doping can be more remarkable since Co may substitute at different spin states, i.e., low spin (LS), intermediate spin (IS), and high spin (HS) states. Some reports on the effect of Co doping on the cubic perovskite manganite have been published [15–18] and a few reports on such studies have also appeared in the case of the bilayered $\text{LaSr}_2\text{Mn}_2\text{O}_7$ manganite prepared by solid state reaction methods [19].

In this paper, we report the effects of low Co doping on the magnetic properties of the $\text{LaSr}_2\text{Mn}_{2-z}\text{Co}_z\text{O}_7$ ($z = 0-0.15$) bilayered manganite prepared by the sol–gel method.

2 Experimental Procedure

$\text{LaSr}_2\text{Mn}_{2-z}\text{Co}_z\text{O}_7$ ($z = 0.00, 0.05, 0.10$ and 0.15) fine powders were prepared by the Pechini sol–gel method. All the chemicals required (analytical grade reagents) were purchased from Merck Company, and used as received without further purification. Highly pure powders of the nitrate precursor reagents $\text{La}(\text{NO}_3)_3 \cdot 6\text{H}_2\text{O}$, $\text{Mn}(\text{NO}_3)_2 \cdot 4\text{H}_2\text{O}$, $\text{Co}(\text{NO}_3)_2 \cdot 4\text{H}_2\text{O}$, and $\text{Sr}(\text{NO}_3)_2$ were weighted in appropriate proportions. The details of experiment was reported in references [20, 21]. The precursors were calcined twice in a Carbolite tube furnace at 1000°C for 10 h and then at 1200°C for 10 h. The black powder obtained was cold-pressed into pellets of 10 mm diameter and thickness of about 2–3 mm under the pressure of 20 ton/cm². Finally, the pellets were sintered for 6 h at 1450°C .

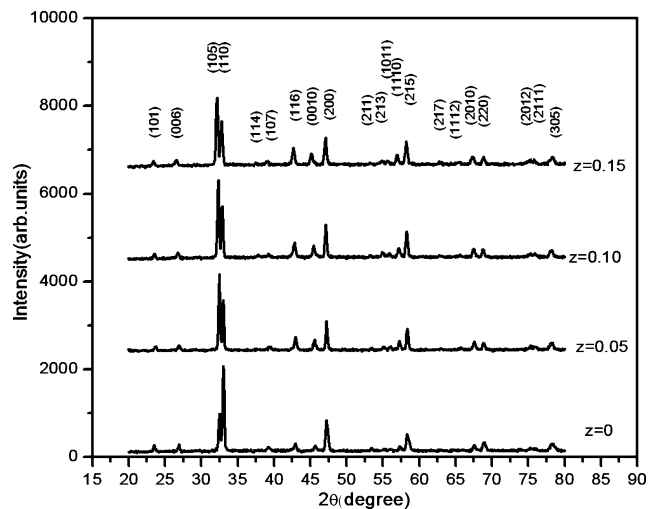


Fig. 1 XRD patterns for the $\text{LaSr}_2\text{Mn}_{2-z}\text{Co}_z\text{O}_7$ ($z = 0.00, 0.05, 0.10,$ and 0.15) samples

Structural properties of the samples were studied by XRD (ADVANCE-D8 model). The ac susceptibility measurements were performed using a Lake Shore Ac Susceptometer Model 7000. The dc magnetization was measured by using SQUID magnetometer. The measurements of Infrared transmission spectra were performed by the IR method using a SHIMADZU FT-IR spectrophotometer model 8400s in KBr pellets.

3 Results and Discussion

3.1 Structural Properties

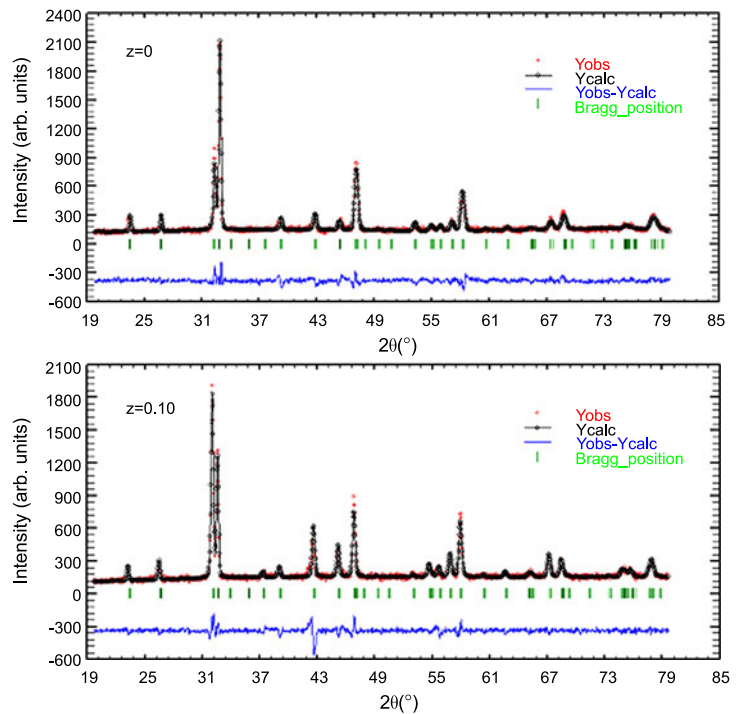
Figure 1 shows the XRD patterns for the samples at room temperature. The XRD data was analyzed with Rietveld refinement using the FULLPROF software and pseudo-Voigt function. It was found that all the diffraction peaks could be indexed using the $\text{Sr}_3\text{Ti}_2\text{O}_7$ -type (327-type) tetragonal structure with $I4/mmm$ space group without any trace of secondary phase or impurity. Co-doping does not change the crystal structure. However, Co-doping affects the Bragg angle position a little that is a common behavior arising from the difference between Mn and Co ionic radii. Rietveld refinement patterns for the samples $z = 0$ and $z = 0.10$ are shown in Fig. 2, and the results of this analysis are collected in Table 1.

As one can see from Table 1 and Fig. 3, there is no systematic change in the lattice parameters of doped samples compared to the parent one. Variation in the observed lattice parameters can be related to the difference in the size of substituted cobalt ions (Co^{3+} (0.61 Å), Co^{4+} (0.54 Å), or even Co^{2+} (0.74 Å)). Also, it should be mentioned that the radius for Mn ions are $\text{Mn}^{3+} = 0.6$ Å and $\text{Mn}^{4+} = 0.53$ Å

Table 1 Lattice parameters, unit cell volume, bond length, and angle obtained from Rietveld refinement

Sample name	<i>a</i> (Å)	<i>c</i> (Å)	<i>c/a</i>	<i>V</i> (Å) ³	Mn–O(1) (Å)	Mn–O(2) (Å)	Mn–O(3) (Å)	Mn–O–Mn (Å)
<i>z</i> = 0.00	3.8575	19.9771	5.1788	297.2654	1.973	1.999	1.967	165.41
<i>z</i> = 0.05	3.8787	20.0415	5.1671	301.5106				
<i>z</i> = 0.10	3.8732	20.0297	5.1714	300.4791	1.975	2.013	1.977	165.98
<i>z</i> = 0.15	3.8526	19.9884	5.1883	296.6784				

Fig. 2 Rietveld profile refinements of the samples *up* (*z* = 0.0) and *down* (*z* = 0.10)



[22]. Therefore, it seems that the possibility of the substitution of Co²⁺ is less than others, although some papers report it for 3D manganites [18, 23–25]. Thus, small cobalt ions compress the neighboring Mn³⁺–O–Mn⁴⁺ bonds, and large cobalt ions stretch the neighboring Mn³⁺–O–Mn⁴⁺ bonds, and this affects the unit cell volume of compounds.

In fact, Co-doping at the Mn site is very complicated. It is possible that in the low doped samples (*z* = 0.05 and 0.10), Co³⁺ ions exist and in other samples Co ions substitute as Co²⁺. The same behavior was reported to occur in the Co-doped 3D manganites La_{0.9}Te_{0.1}Mn_{1-x}Co_xO₃ (0 < *x* < 0.25) by Zheng and coworkers [18].

FT-IR spectra for samples are shown in Fig. 4. MnO₆ in the crystalline structure of manganite has nearly ideal octahedral symmetry with six vibration modes, but only two of them are IR-active. The band around 600 cm⁻¹ corresponds to the stretching mode (*ν*₃) of Mn–O–Mn or Mn–O bonds, while the bending mode (*ν*₄) around 400 cm⁻¹ is due to changes in the Mn–O–Mn bond angle [26–30].

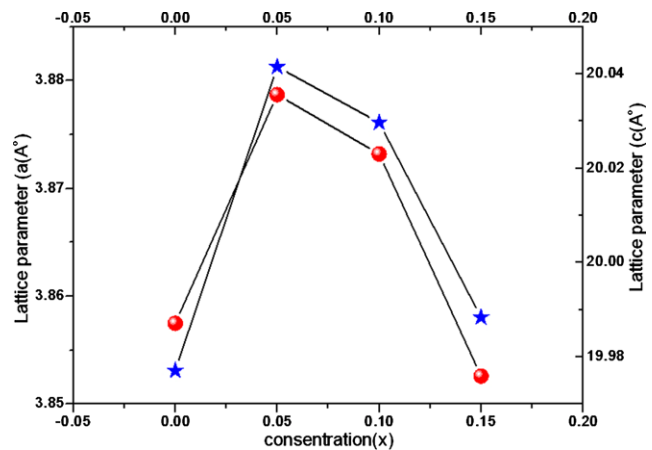


Fig. 3 The lattice parameters (*a* and *c*) versus Co-doping level (*x*)

Appearance of the stretching and bending modes in the transmission spectra for all samples indicate that the structure of manganites is formed. It is worth mentioning that a shift and splitting is seen in the transmission spectra of

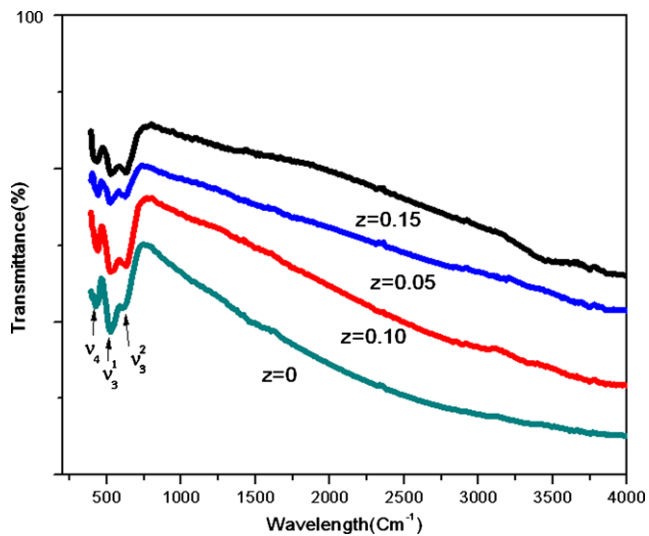


Fig. 4 The FT-IR spectra of samples

Table 2 The stretching and bending modes of samples

Samples	ν_3 (cm^{-1})		ν_4 (cm^{-1})
	ν_3^1	ν_3^2	ν_4
$z = 0.00$	525	613	429
$z = 0.05$	519	630	436
$z = 0.10$	525	633	438
$z = 0.15$	528	635	433

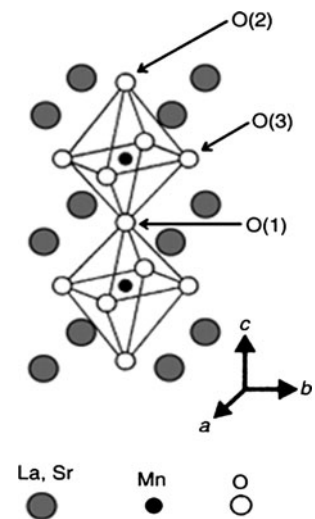
samples. The stretching and bending modes of samples are collected in Table 2.

As one can see, there is a shift in wavelength of the bending mode as well as a splitting in stretching mode. It seems that, by the increasing of doping level, the splitting enhances more. There are some reports about the stretching mode shifting to a lower wave number [28, 30, 31], and they have attributed this to the Jahn–Teller effect caused by the Mn^{3+} ion.

In layered manganites with a tetragonal space group $I4/mmm$, oxygen resides in three positions labeled; Mn–O(1), Mn–O(2), Mn–O(3), (see Fig. 5) [2]. The structural study of single crystal half-doped layered manganites ($\text{LaSr}_2\text{Mn}_2\text{O}_7$) showed that all Mn–O bonds lengths are the same [2], however, it seems there is difference between Mn–O bonds lengths in polycrystalline samples of $\text{LaSr}_2\text{Mn}_2\text{O}_7$ [14, 32].

In doped samples, cobalt cations would be settled randomly over octahedral positions. Due to the changing of cobalt ions sizes with valance, the structure of the compound experiences distortion because of tilt in octahedra. So, the length of (Mn, Co)–O(1), (Mn, Co)–O(2), and (Mn, Co)–O(3) bonds change and probably the (Mn, Co)–O(2) changing is remarkable, because this oxygen resides in the out of

Fig. 5 Oxygen positions in layered manganites (O(1), O(2), O(3)) [2]



the plane. According to ν_3 and ν_4 values, it can be deduced that the stretching mode changes more remarkably than the bending mode. So, cobalt substitution changes the lengths of the bonds and the variation of ν_3 and ν_4 values indicate a strong coupling between (Mn, Co)–O vibration frequency with the bond lengths. These results support the XRD results discussed above. So, these results may reflect JT distortion, due to the fact that the JT distortion basically influences the MnO_6 octahedra.

3.2 Magnetic Properties

As mentioned in the Introduction section, recent reports [10] show CE-type CO and A-type AFM spin ordering occurs below 210 K in the $\text{LaSr}_2\text{Mn}_2\text{O}_7$ compound. The ground state is the CE-type, and the AFM phase appears at 145 K [8]. The CE-type charge ordering is expected to be favored in the localized $d_{3x^2-r^2}/3y^2-r^2$ type orbital order. In the half-doped manganite case, Mn^{3+} and Mn^{4+} ions are ordered alternately in the MnO_2 bilayers and the orbital of the additional e_g electron at the Mn^{3+} site becomes ordered in the checkerboard (zigzag) pattern [7], while the A-type one is in the metallic $d_{x^2-z^2}/y^2-z^2$ type order. For this reason, generally, the CE-type system is insulating, and in contrast, the A-type system has a metallic behavior.

For investigation of the magnetic phase transition, the ac magnetic susceptibility, $\chi(T) = \chi' + i\chi''$, measurements were performed in the weak magnetic field of rms strength 10 Oe, and at a frequency of 333 Hz. Figure 6 shows temperature dependence of the ac susceptibility for the samples.

Actually, an oscillating magnetic behavior can be seen as a few peaks above CO transition around $T_{\text{CO}} = 220$ K in the high temperature, in the paramagnetic phase for the parent compound. The amplitude of these oscillations increases near the CO phase, and they disappear in the CO phase. The origin of this strange behavior has

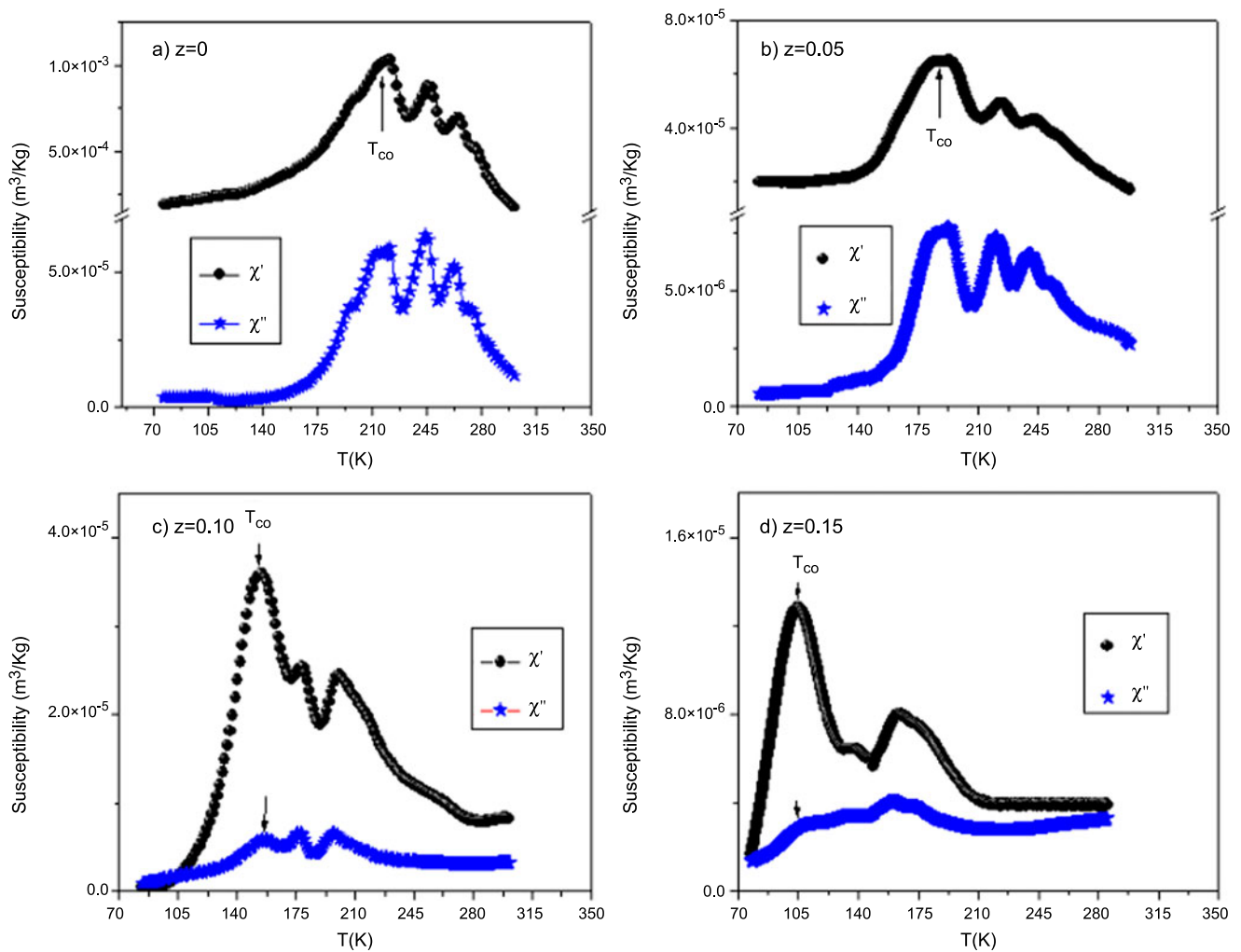


Fig. 6 Ac susceptibility versus temperature plots for the samples

not understood yet, but it has previously been reported for single crystal compounds $\text{La}_{1+x}\text{Sr}_{2-x}\text{Mn}_2\text{O}_7$ ($x = 0-0.4$), $\text{La}_{1.2}(\text{Sr}_{1-x}\text{Ca}_x)_{1.8}\text{Mn}_2\text{O}_7$, $\text{La}_{1.2}\text{Sr}_{1.8}\text{Mn}_2\text{O}_7$, and $\text{La}_{1.33}\text{Sr}_{1.66}\text{Mn}_2\text{O}_{7.12}$ [6, 33–35]. It has been predicted that rotation of Mn spins probably creates such an unusual behavior. Mitchell et al. have stated that this feature does not originate from the impurity phase since the single layer $(\text{La}, \text{Sr})_2\text{MnO}_4$ compounds are paramagnetic at $T > 150$ K [6], and they believe it is related to the spin correlations on a short-range length scale, and might be intrinsic to this class of 2D materials.

In Figs. 6(a)–(d), one can clearly see the effect of Co-doping on the real $\chi'(T)$ and imaginary $\chi''(T)$ parts of ac susceptibility for the samples. Co-doping destroys the ordering arrangement of Mn^{3+} and Mn^{4+} ions, resulting in weakening of the AFM state in $\text{LaSr}_2\text{Mn}_2\text{O}_7$. T_{CO} decreases from 220 K ($z = 0$) to 102 K ($z = 0.15$). Also, although the pattern of oscillating behavior is changed by Co doping, but this

behavior still exists in the paramagnetic background even in $z = 0.15$ sample.

For further investigation of the oscillating behavior, we focus on the $z = 0$ sample and the susceptibility measurement under the extra applied dc field was carried out.

As one can see in Fig. 7, the amplitude of the oscillating trend is decreased by the dc applied field. So, this behavior should not come from structural inhomogeneity or defects. As Wu and coworkers [33] have predicted, this behavior may be related to rotation of Mn spins. A weak dc applied field may pin the Mn spins and the oscillating behavior disappears but not completely.

For further study and getting the magnetic information, the dc magnetization $M(T)$ for the parent sample was also carried out in both Zero-field-cooling (ZFC) and field-cooling (FC) modes at an applied magnetic field of 50 Oe, 100 Oe, and 1000 Oe.

Figure 8 shows the temperature dependence of magnetization ($M-T$), field dependence of magnetization ($M-H$)

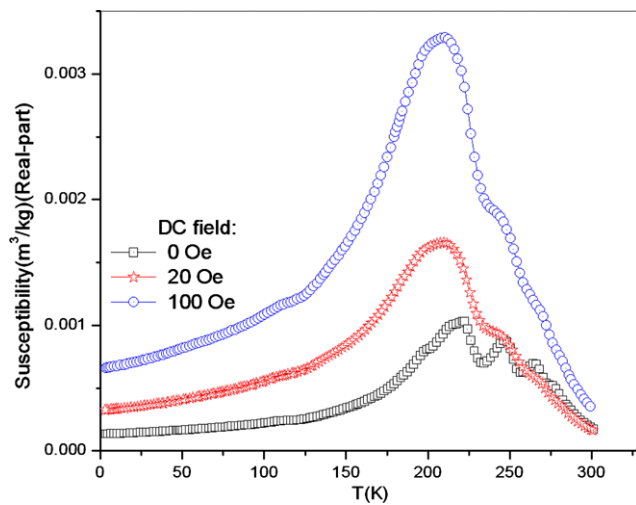


Fig. 7 Real part of ac susceptibility versus temperature at dc applied field (0, 20, 100 Oe) for the $z = 0$ sample

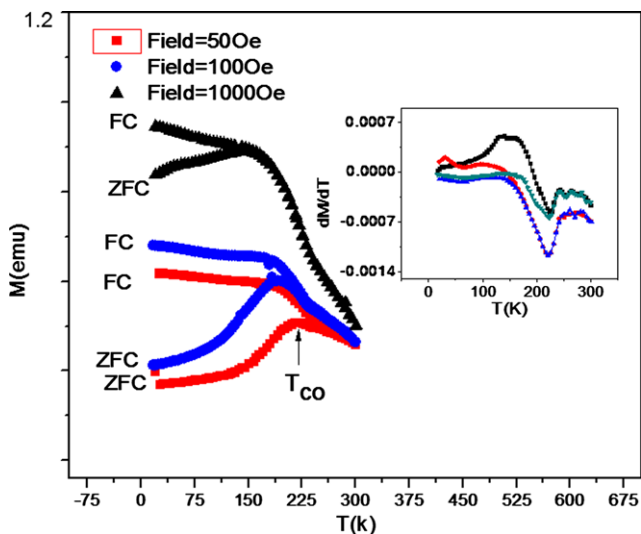


Fig. 8 Temperature dependence of FC and ZFC magnetization, and (inset) dM/dT for $z = 0$ sample

measured at a few selected temperatures, as well as differential of magnetization (dM/dT) for the parent sample.

By decreasing the temperature, the ZFC curve shows a peak about ~ 225 K in applied field of 50 Oe corresponding to the T_{CO} . The peak shifts to lower temperatures by increasing of the magnetic field strength. As one can see in Fig. 9, the hysteresis loop measurements at some selected temperatures indicate that the magnitude of magnetization increases drastically in low applied fields and does not reach saturation up to 5 Tesla, indicating the existence of AFM background in this sample. Also, one can observe that by increasing the applied field the discrepancy of ZFC and FC decreases. This means that there is an AFM interaction competing with the dominant FM interaction. Also, the observed

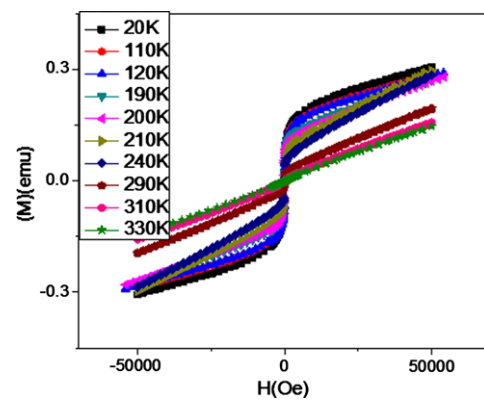


Fig. 9 Field dependence of magnetization for the $z = 0$ sample

weak ferromagnetic hysteresis loops at 20 K and 110 K is related to interlayer FM interactions.

The results of dc magnetization are in agreement with our ac susceptibility results. From dc magnetization measurements, we can claim the oscillating behavior still exists. The dM/dT versus T curves, which is shown in the inset of Fig. 8, confirms this opinion.

To the best of our knowledge, there is not any exact explanation for the origin of this anomalous behavior. In our study, the FT-IR results confirm the existence of distortion in crystal structure of samples so that it increases by increasing the cobalt doping level. The results of our ac susceptibility measurement under a weak dc applied field and dc magnetization show that probably the rotation of Mn ions spins and fluctuation in short range ordering of them can cause this oscillating behavior. So, it seems that although the origin of this behavior is not obvious; however, it may be concluded that this behavior is an intrinsic nature in layered manganites as Mitchell has stated regarding these materials [6].

4 Conclusion

The $\text{LaSr}_2\text{Mn}_{2-z}\text{Co}_z\text{O}_7$ ($z = 0-0.15$) polycrystalline compounds were synthesized by the sol-gel method. The Rietveld refinements of samples show that all adopt a $\text{Sr}_3\text{Ti}_2\text{O}_7$ -type (327-type) perovskite structure. FT-IR studies show a small splitting in the stretching mode for the undoped sample and a clear splitting is seen for doped samples. These are due to distortion in the crystal structure caused by the Jahn-Teller effect. The ac and dc magnetic measurements by Susceptometer and Squid equipment exhibit an antiferromagnetic phase transition, which is accompanied by charge ordering state occurs around 220 K for an undoped sample and it shifts to lower temperatures by increasing the CO doping level. The ac susceptibility measurements show an anomalous oscillating behavior. This behavior is suppressed by increasing the CO doping level, but does not completely disappear. The amplitude of these oscillations is reduced by ap-

plying the dc field. Therefore, the oscillating behavior may be due to the Mn spin rotation and fluctuation in short range spin ordering and is an intrinsic nature of layered manganites and not caused by impurity.

References

- Kimura, T., Tomioka, Y., Kuwahara, H., Asamitsu, A., Tamura, M., Tokura, Y.: *Science* **274**, 1698 (1996)
- Kimura, T., Tokura, Y.: *Annu. Rev. Mater. Sci.* **30**, 451 (2000)
- Zener, C.: *Phys. Rev.* **82**, 403 (1951)
- Dagotto, E., Hotta, T., Morea, A.: *Phys. Rep.* **344**, 1 (2001)
- Osborn, R., Rosenkranz, S., Argyriou, D.N., Vasiliu-Doloc, L., Lynn, J.W., Sinha, S.K., Mitchell, J.F., Gray, K.E., Bader, S.D.: *Phys. Rev. Lett.* **83**, 3964 (1998)
- Mitchell, J.F., Argyriou, D.N., Jorgensen, D.J.D., Hinks, D.G., Potter, C.D., Bader, S.D.: *Phys. Rev.* **55**, 63 (1997)
- Goodenough, J.B.: *Phys. Rev.* **100**, 564 (1955)
- Kubota, M., Yoshizawa, H., Moritomo, Y., Fujioka, H., Hirota, K., Endoh, Y.: *J. Phys. Soc. Jpn.* **68**, 2202 (1999)
- Li, Q.A., Gray, K.E., Zheng, H., Claus, H., Rosenkranz, S., Ancona, S.N., Mitchell, J.F., Chen, Y., Lynn, J.-W.: *Phys. Rev. Lett.* **98**, 167201 (2007)
- Lee, J.S., Kao, C.C., Nelson, C.S., Jang, H., Ko, K.T., Kim, S.B., Choi, Y.J., Cheong, S.W., Smadici, S., Abbamonte, P., Park, J.H.: *Phys. Rev. Lett.* **107**, 037266 (2011)
- Yu, G.Q., Wang, Y.Q., Liu, L., Yin, S.Y., Ren, G.M., Miao, J.M., Xiao, X., Yuan, S.L.: *Solid State Commun.* **141**, 136 (2007)
- Yu, G., Xu, B., Xiong, J., Liu, X., Liu, L., Yuan, S.: *J. Magn. Magn. Mater.* **323**, 1925 (2011)
- Zhu, H., Xu, X., Pi, L., Zhang, Y.: *Phys. Rev. B* **62**, 6754 (2000)
- Nair, S., Banerjee, A.: *Phys. Rev. B* **70**, 104428 (2004)
- Ying, Y., Eom, T.W., Dai, N.V., Lee, Y.P.: *J. Magn. Magn. Mater.* **323**, 94 (2011)
- Srivastava, S.K., Kar, M., Ravi, S.: *J. Magn. Magn. Mater.* **320**, e107 (2008)
- Moreno, N.O., Campoy, J.C.P., Blanco, J.J., Insausti, M., Rojo, T., Barberis, G.E.: *J. Magn. Magn. Mater.* **226–230**, 834 (2001)
- Zheng, G.H., Sun, Y.P., Zhu, X.B., Song, W.H.: *Solid State Commun.* **137**, 326 (2006)
- Zhang, R.L., Song, W.H., Ma, Y.Q., Yang, J., Zhao, B.C., Sheng, Z.G., Dai, J.M., Sun, Y.P.: *Phys. Rev. B* **70**, 224418 (2004)
- Ehsani, M.H., Kameli, P., Ghazi, M.E.: *J. Phys. Chem. Solids* **73**, 744 (2012)
- Ehsani, M.H., Ghazi, M.E., Kameli, P.: *J. Mater. Sci.* **47**, 5815 (2012)
- Shannon, R.D.: *Acta Crystallogr., Sect. A* **32**, 751 (1976)
- Yu, Q., Zhang, J., Jia, R., Jing, C., Cao, S.: *J. Magn. Magn. Mater.* **320**, 3313 (2008)
- Ying, Y., Eom, T.W., Dai, N.V., Lee, Y.P.: *J. Magn. Magn. Mater.* **323**, 94 (2011)
- Joy, P.A., Kholam, Y.B., Date, S.K.: *Phys. Rev. B* **62**, 8608 (2002)
- Nagabhushana, B.M., Sreekanth Chakradhar, R.P., Ramesh, K.P., Prasad, V., Shivakumara, C., Chandrappa, G.T.: *Physica B* **403**, 3360 (2008)
- Li, K., Cheng, R., Wang, S., Zhang, Y.: *J. Phys. Condens. Matter* **10**, 4315 (1998)
- Kebin, L., Xijun, L., Kaigui, Z., Jingsheng, Z., Yuheng, Z.: *J. Appl. Phys.* **81**, 6943 (1997)
- Rostamnejadi, A., Salamati, H., Kameli, P.: *J. Supercond. Nov. Magn.* **25**, 1123 (2012)
- Zhang, T., Li, G., Qian, T., Qu, J.F., Xiang, X.Q., Li, X.G.: *J. Appl. Phys.* **100**, 094324 (2006)
- Oumezzine, M., Pena, O., Guizouarn, T., Lebullenger, R., Oumezzinehys, M.: *J. Magn. Magn. Mater.* **324**, 2821 (2012)
- Sehadri, R., Maignan, A., Hervieu, M., Nguyen, N., Raveau, B.: *Solid State Commun.* **101**, 453 (1997)
- Wu, S.Y., Li, W.-H., Lee, K.C., Yang, H.D.: *Physica B* **259–261**, 839 (1999)
- Ganguly, R., Siruguri, V., Gopalakrishnan, I.K., Yakhmi, J.V.: *J. Phys. Condens. Matter* **12**, 1683 (2000)
- MacChesney, J.B., Potter, J.F., Sherwood, R.C.: *J. Appl. Phys.* **40**, 1243 (1969)